

1 **Large-scale shoreline undulations and role of self-organization**
2 **processes**

3 Xiaojing Zhong^{a*}, Ping Dong^{b*}, Shenliang Chen^{c**}

4 ^a*School of engineering and Technology, Jimei University, Xiamen 361021, China*

5 ^b*School of Engineering, University of Liverpool, Liverpool L69 3BX, United Kingdom*

6 ^c*State Key Laboratory of Estuarine and Coastal Research, East China Normal University, Shanghai*
7 *200062, China*

8 * These authors contributed equally to this work.

9 **Corresponding author: slchen@sklec.ecnu.edu.cn

10

11 **ABSTRACT**

12 This study investigates the large scale spatial variation behavior of shoreline changes
13 using the beach profile data along approximately 600 km shoreline around Hainan
14 Island, China. It is found that there exists a power-law relationship between the mean
15 shoreline change variance and the corresponding alongshore scale which holds up to
16 30 km for the annual shoreline change and reduces to 15 km for seasonal shoreline
17 change. The spatial and seasonal variations of shoreline azimuth, beach sediment size
18 and wave conditions, and their connection with the shoreline change on different
19 scales have been studied. The results suggest that the internal feedback mechanisms
20 between various processes with different spatial scales may be responsible for the
21 observed shoreline change patterns, i.e. the annual shoreline behavior on spatial scale
22 5-30 km is likely to be the result of self-organization, while the seasonal waves

23 including tropical cyclones and storms exert dominant control of the morphological
24 patterns at spatial scale of 10-25 km.

25

26 **ADDITIONAL INDEX WORDS:** beach; self-affinity; power-law; forcing; seasonal.

27

28 **Introduction**

29 Coastal evolution involves complicated interactions and often exhibits self-similar
30 (self-affine, fractal) patterns, which can be characterized by power-law scalings. The
31 forms of these patterns are numerous (*e.g.*, beach cusps¹, sand-bars^{2,3}, rip-channels⁴,
32 and large scale shoreline patterns⁵) and vary in a wide range of spatiotemporal scale.

33 Self-organized processes whose outcomes exhibit power-law scaling, are often
34 observed and applied for modeling^{1, 2, 6} and can be easily explained if the spatial
35 scales involved are relatively small. However, the power-law scaling that spans over
36 wide range of scales is much harder to interpret due to the self-organized patterns at
37 different scales may be controlled by different physical processes. This means an
38 unifying explanation for the relationship between variances of coastal morphological
39 changes, such as horizontal movement of shoreline⁷ or change of shoreline curvature⁸
40 is presently not available. Therefore, to establish the scale relationships of
41 morphological changes on coasts and underlying mechanisms for these changes,
42 investigations of coastal evolution in a wider range of scales is indispensable. In
43 addition, a better understanding on the connection between power-law scaling and
44 morphological self-organization on coast will be promoted accordingly.

45 While there exists a comparatively large amount of research on forced coastal

46 forms, the self-organized behavior of coastal morphology in a wide range of scales
47 still needs further exploration and research⁹. Based on analysis of cross-shore profile
48 changes in terms of their self-organizational properties, Southgate and Moller¹⁰ found
49 that when wave conditions were weak or moderate, self-organizational (internal)
50 processes determined the dynamics of the beach profile. The work of Tebbens,
51 Burroughs, and Nelson⁷ focused on the shoreline change for tens of kilometers along
52 of the northern North Carolina Outer Banks, United States. The log-log linear
53 relationship between alongshore scale and the variance of horizontal shoreline
54 position change in the cross-shore direction was found to hold for alongshore scales
55 of approximately 100-1,000 m, and a follow-on study by Lazarus *et al.*⁸ has extended
56 the scale to up to 8 km. These findings are important as it means that cumulative
57 shoreline evolution process over a period of a year or a few years may exhibit
58 power-law scalings up to a length of 8 km although the underlying processes are
59 unlikely to be scale free.

60 In this work, the power-law behavior of shoreline changes at large spatial scales is
61 investigated, and possible mechanisms to explain this behavior are explored. The data
62 of horizontal shoreline position change on beach profile used for this study are
63 obtained from three beach profile surveys conducted in a 13-month period along the
64 entire 600 km shoreline around Hainan Island, China. Wavelet analysis are applied to
65 identify the power-law behavior of horizontal shoreline position change and
66 distinguish the shoreline change characteristics at different spatial scale. The standard
67 Empirical Orthogonal Function (EOF) analysis is applied on the elevation data of

68 beach profile to study the variation characteristics of beach morphology in cross-shore
69 direction at various coastal sections, and the analysis results are discussed along with
70 a set of hydrodynamic and geologic conditions in order to shed further light on the
71 underlying mechanisms for the observed shoreline change patterns.

72

73 **Study area**

74 Hainan Island is located in the South China Sea, separated from Leizhou
75 Peninsula to the north by Qiongzhou Strait (Figure 1). Due to engineering works and
76 urban development at Hainan Island, water and sediment fluxes of rivers on the island
77 decreased slowly in recent 50 years¹¹. At present, sediments involved in the coastal
78 evolution around Hainan Island mainly originate from the resuspension of deposited
79 sediment and the erosion of backshore dunes¹². Sandy coasts are the main shoreline
80 types, and they are separated by bedrock headlands and estuaries (Figure 1 and Table
81 1). From Hainanjiao to Laoyehai is the east coast with shoreline facing east, and from
82 Laoyehai down to Yinggeju is the south coast.

83 The climate of Hainan Island and South China Sea is dominated by the East
84 Asian monsoon, with northwest winds during October-March (winter), and south and
85 southeast winds during April-September (summer)^{12, 13}. The direction and energy of
86 surface waves around the island are also closely correlated with the seasonal wind
87 direction and forcing strength¹². Prevailing waves are from northeast in winter and
88 southeast and southwest in summer. In summer season, the Hainan Island is
89 frequently visited by tropical cyclones (about 3 times per year¹⁴).

90

91 **Methods**

92 **Field survey and data**

93 132 profiles perpendicular to local shoreline around Hainan Island are surveyed,
94 and the distance between every two adjacent profiles is approximately 5 kilometers
95 (Figure 1). Profile elevation measurements were taken with Trimble RTK-GPS 3
96 times in May 2013 (from 30th April to 14th May, 2013), Dec 2013 (from 6th December
97 to 21st December, 2013) and Jun 2014 (from 6th June to 20th June, 2014). The
98 measuring error is less than 6 cm, which is much smaller than the magnitude of
99 shoreline position variations involved. The latitude and longitude of each profile are
100 recorded in the first survey, and then precisely located in the subsequent surveys.
101 Mean sea level (MSL, 0-m contour) is taken as the representative shoreline position
102 which can be easily and accurately determined by beach survey data¹⁵. The difference
103 between the distances from the fixed measuring points at the backshore of the profiles
104 to MSL of the two surveys is then taken as the shoreline change. Among the three sets
105 of data for comparison, May2013-Jun2014 (difference of shoreline position between
106 Jun 2014 and May 2013) represents the annual variation of shoreline while
107 May2013-Dec2013 and Dec2013-Jun2014 are the seasonal changes of shoreline.

108 For each profile measured, five sediment samples were collected along the beach
109 profile starting 2 cm from the top of the profile in the first survey. Sieve analysis is
110 used to obtain particle size distributions of the samples, and the Friedman series
111 formulas¹⁶ are then employed to determine the median grain size (D_{50}) of each

112 sediment sample. D_{50} values from the same profile are averaged to represent the
113 sediment size for the profile.

114 **Shoreline change analysis**

115 The changes in the MSL positions at 132 profiles constitute the shoreline change
116 series around Hainan Island with missing data being filled by linear interpolation. The
117 data is then reconstructed by wavelet transform, which provides information on both
118 the spatial and frequency dependence of a data series. The wavelet analyses are
119 performed using the Wavelet Toolbox in Matlab R2010a. A filter called the Mexican
120 hat wavelet convolves with shoreline change signal, and values for the scale
121 parameter, a , are within the range from 1 to 16. Since the profiles are distributed one
122 after another around the Hainan Island, there is no beginning or ending of the
123 shoreline change signal in the true sense. The profiles are named N001 to N132, and
124 then the term N001 to N132 are repeated three times in sequence to form the signal
125 used for wavelet transform, that is: N001, N002 ... N132, N001, N002 ... N132,
126 N001, N002 ... N132. Only the middle part of coefficient series obtained is used, so
127 that the results are not affected by the edge effect of wavelet transform. The
128 power-spectral exponent, β , is the slope of log-log plot of the variance of wavelet
129 transform coefficients, V , and the wavelet scale, a .

130 **Beach profiles analysis**

131 The EOF analysis is applied to investigate beach profile features of different
132 coastal sections in different time. Each profile is transformed into a set of elevation
133 data with a spatial interval of 1.5 m, starting from MSL. For unifying the length of

134 different profiles, the landward blank elevation data are filled with the elevation of the
135 farthest point measured, which usually is the highest point for those shorter profiles.
136 Hence there are 100 elevation variables on each profile while the unified profile
137 length is 150 meters. The 132 profiles, each with 100 elevation variables, constitute a
138 multivariate matrix fed to the EOF analysis. For unified profile elevation data from
139 the same survey, four beach topography data matrixes used for the EOF analysis are
140 obtained: one matrix contains all the profiles around Hainan Island (N001~N132), and
141 three matrixes for east coast (N010~N049), south coast (N049~N087) and the north &
142 west coast (N088~N009) separately. In total 12 matrixes are generated for three
143 surveys. The calculation procedures followed closely the work of Vincent *et al.*¹⁷.

144 **Hydrodynamic and geological conditions**

145 Routes of tropical cyclones are accessed from Best Track Data by RSMC Tokyo -
146 Typhoon Center (www.jma.go.jp). Significant wave height and wave direction around
147 Hainan during the investigated period are accessed from hourly forecast data of
148 WaveWatch III (WW3) Global Wave Model (oos.soest.hawaii.edu/erddap), which has
149 taken account of the weather conditions including tropical cyclones. While the
150 resolution of WW3 Global wave model is 0.5 degree of longitude/latitude, the
151 modeling points of wave conditions are mostly located in deep water or far away from
152 the shoreline. Therefore, in analyzing the wave effects on the shoreline change
153 patterns, the seasonal significant wave heights along coast of Hainan predicted by
154 Zhou *et al.*¹⁸ is also used.

155 Since the surveyed beach profiles are perpendicular to local shoreline, the

156 azimuths of these investigated profiles can represent the orientation of the local
157 shoreline around Hainan Island. Azimuths of investigated profiles are calculated from
158 GPS data. To examine the spatial scale of shoreline orientation variation along the
159 coast, wavelet transform is used to analyze the azimuth data series.

160

161 **Results**

162 **Rhythmic shoreline changes at different scales**

163 Shoreline change signals exhibit a rhythmic pattern of alternating seaward and
164 shoreward movements alongshore (Figure 2(a)). At most survey positions, the
165 shoreline moves in opposite directions in the two seasons (May2013-Dec2013 and
166 Dec2013-Jun2014) considered. The contrast between the wavelet transformed results
167 of two seasonal shoreline change signals is also clearly evident (Figure 2(b) and 2(c)):
168 the coast which moved shoreward from summer to winter (May2013-Dec2013)
169 usually changed to moving seaward from the winter to the following summer
170 (Dec2013-Jun2014), and vice versa. The spatial periodic variations in the shoreline
171 change series are clearly strong on different spatial scales.

172 The variations of shoreline change signals at different sections around Hainan
173 Island are quite different as shown in Figure 2. The shaded parts are the south & east
174 coast, and the cyclic variation there is more pronounced than the rest. In other words,
175 the shoreline at south & east coast is more unstable than north & west coast, except
176 the three abnormal profiles (Figure 2(a)): N104, N118 and N123. Profiles N104 and
177 N123 have underwater shoal and mangrove, which may cause large changes in the

178 local shoreline position. As to profile N118, it is affected by an artificial island located
179 besides it, which was newly built after the first survey. Other profiles at north & west
180 coast did not change much in shoreline position. Subsequent discussion will put
181 particular emphasis on the south & east coast (profiles N010-N087).

182 **Relationships between wavelet coefficient variance and spatial scale of shoreline** 183 **changes**

184 The relationships between the wavelet transform coefficient variance and the
185 spatial scale of shoreline change series at south & east coast are shown in Figure 3 by
186 log-log plots. In the left graph, the wavelet coefficient variance of annual shoreline
187 change, May2013-Jun2014, rises continually at alongshore scale from 5 km to 30 km,
188 and increases again in the scale range of 60-80 km after dropping at 35-60 km. In
189 contrast the rising trends of seasonal change series, May2013-Dec2013 and
190 Dec2013-Jun2014, break off in the scale range of 10-25 km, and then increase again
191 up to scale around 60 km. The power-spectral exponent, β , of annual shoreline change
192 is steady over the scale range of 5-30 km. The power-law relationships of seasonal
193 shoreline change are also strong with exponent β larger than 1 in the spatial scale up
194 to 15 km.

195 **Cross-shore profile change characteristics**

196 The EOF analysis reveals that first and second eigenvectors can explain over 90%
197 variation of profile elevation (Table 2). The first eigenvectors show the prevailing
198 beach profile forms, and the second eigenvectors reflect the subsequent beach
199 elevation changes along the profiles. In Figure 4(b) and 4(c), it can be clearly seen

200 that the shapes of eigenvectors of winter profiles (Dec2013) are quite different from
201 that of summer profiles (May2013 and Jun2014) for all profiles, which implies
202 seasonal morphological changes on Hainan coasts.

203 The large variation of eigenvector weighting also indicates significant changes of
204 beach profile, *e.g.* the second eigenvector weightings of profiles from N40 to N70
205 vary notably between surveys (Figure 4(a)). On the other hand, profiles alongshore
206 with close eigenvector weightings suggest they have similar relationships with
207 eigenvector. Therefore subsections of coast can be recognized by differences in the
208 weightings on alongshore profiles, and the coastal sections divided on this basis
209 corresponds well with the geological conditions (Table 1).

210 **Hydrodynamic conditions**

211 For the south & east coast of Hainan, the direction of incident wave in deep water
212 is almost uniform alongshore with no discernable rhythmic patterns as it can be seen
213 in Figure 1. Furthermore, the annual significant wave height distribution in the coastal
214 area considered is also rather similar, varying within the range of 0.6-1.2 meter
215 (Figure 5 (a)). As shown in Figure 1, along the east and south coast of Hainan, the
216 prevailing wave direction is east-northeast in two seasons, while a proportion of
217 waves coming from south in May2013-Dec2013 changes to east in Dec2013-Jun2014.

218 During the survey period, there were five tropical cyclones that passed Hainan
219 Island (Figure 1 and Table 3). All these cyclones approached Hainan from the east and
220 south coasts between surveys in May 2013 and Dec 2013, and the last cyclone passed
221 east coast was 4 months before the survey in Dec 2013 while the last cyclone affected

222 south coast only 25 days before 6th Dec 2013. Among the five cyclones, HAIYAN is
223 the strongest and largest one (Table 3), and all of them are strong enough to affect the
224 hydrodynamic conditions at some parts of Hainan coast. The cyclones generated high
225 waves over a wide area, which can be recognized from wave conditions on both
226 southeast coast and west coast (Figure 5(b) and 5(c)). Based on the modelling wave
227 conditions in 18.5°N, 110.5°E (*P1*) and 19°N, 108.5°E (*P2*), it can be concluded that
228 the survey in Dec 2013 was affected by waves with relatively higher significant wave
229 height induced by a series of storms, while the surveys in May 2013 and Jun 2014
230 were taken after a prolonged period of low waves.

231 **Geological conditions**

232 As shown in Figure 1, most profiles in the survey are on sandy beaches, only a
233 few of them are covered by very fine gravel. It can also be found that the sediments
234 from each single bay are nearly of the same size, but differ significantly from that in
235 the adjacent bays. The bays with alongshore length around 30-40 km are separated by
236 protruding shoreline. As it can be seen in Figure 6, at the spatial scales under 20 km,
237 the variation trends of shoreline change and azimuth are very different from one
238 another (Figure 6(a)), and the Pearson product-moment correlation coefficient
239 between them is only 0.21, which means they are barely correlated. At scale of 40 km
240 alongshore the correlation is more discernible but remains weak (Figure 6(b)) while at
241 scale of 80 km alongshore (Figure 6(c)), the azimuth displays similar trends with
242 shoreline change signal.

243

244 **Discussion**

245 The phenomena that shoreline changes driven by seemingly different processes
246 can exhibit a consistent trend across a wider range of scales in a power spectrum is
247 indeed both interesting and hard to explain. Compared with the previous studies^{7, 8, 19},
248 the scale of the present study area is much larger. The power-law relationship for the
249 annual data implies that the self-affine property of shoreline changes can exist over
250 four orders of magnitude in alongshore scale, from 10 meters to 3×10^4 meters. As
251 this wide range of scales covers most spatial scales pertaining to the short and
252 medium term coastal evolution, the results suggest that shoreline movements within
253 these scales could be strongly affected by nonlinear shoreline change dynamics
254 including some forms of self-organization.

255 Since the concept of “self-organization” was introduced by Werner and Fink¹ in
256 their study of beach cusps, models involving self-organization have largely focused
257 on the explanation for the formation of rhythmic features at specific spatial scales,
258 from meters to over 100 km under a prescribed background hydrodynamic
259 conditions²⁰. It remains unclear how the self-organization or a combined forced and
260 self-organization mechanism may be used to explain the dynamical changes of
261 shorelines that exhibit power-law scaling²¹. The shoreline change patterns around
262 Hainan Island revealed in this study may provide useful information about spatial and
263 temporal boundaries between self-organization and forcing processes.

264 **Self-organization behavior of coastal morphology**

265 For a complex system involving many processes with different scales which

266 interact on the overlapping spatial scales, the peaks of the shoreline-change power
267 spectra occurring at specific scales may indicate a possible transition of dominant
268 processes but this does not preclude the possibility of a well-organized system with
269 different processes across different scales. For temporal scale one year and spatial
270 scale up to 30 km (May2013-Jun2014), the shoreline change seems to be a result of
271 well-organized system with smooth growth of spectra power along with scales, while
272 the strong seasonal hydrodynamic conditions can cause this trend to break in temporal
273 scale of half year and spatial scale 10-25 km. The evaluation of affecting
274 factors/processes, weak or strong, relies on the temporal and spatial scales considered.

275 Within alongshore scale 5-30 km, none of azimuth, sediment or deep water wave
276 shows strong correlations with shoreline change (Figure 1 and 6, east and south coast).
277 This indicates that there does not exist a dominant process that is due to any of these
278 factors in the system. The system evolves mainly through internal feedback
279 mechanisms between processes with different spatial scales, *i.e.* through
280 self-organization. And the peaks of spectrum around scale 30 km and beyond are
281 more likely due to other controlling factors of the system.

282 **Controlling role of seasonal hydrodynamic conditions at the scale of 10-25 km**

283 Based on the modelling wave data, tropical cyclones can generate high waves
284 over a large sea surface area: distance between *P1* and *P2* is more than 200 km but
285 high waves driven by cyclones can be easily identified in both positions. The
286 shoreline change in May2013-Dec2013 shows little erosion on east coast, only a part
287 of south coast is seriously eroded. This may be due to the time intervals between the

288 tropical cyclones and the survey, because the cyclones impacted east coast 4 months
289 before the survey in December and their effects have diminished as the result of beach
290 recovery during this period, but the last storm passed south coast in November which
291 is expected to leave a much greater impact on shoreline measured in December.

292 As it can be expected, high waves induced by cyclones and winter storms can
293 destroy shoreline patterns that had already formed through self-organization process
294 prior to these events after which beach recovery and evolution will resume. This is
295 especially the case for the shoreline changes in May2013-Dec2013 data. As through
296 self-organization process spatial shoreline patterns tend to grow with time, larger
297 scale pattern requires longer time to form than smaller ones²⁰. Although there are 1-4
298 months for shoreline to recovery from impacts of tropical cyclones by Dec 2013, only
299 smaller (less than 10km) shoreline change patterns developed but larger patterns
300 beyond 10km did not have sufficient time to form until Jun 2014.

301 **Geological control at the scales over 30 km**

302 Apart from self-organization and hydrodynamic forcing, the changes in the
303 background coastal settings can also affect the evolution of shoreline, an effect which
304 is often referred to as geological control²². Although the correlation is weak between
305 data sets of shoreline change and azimuth, the variation patterns of them do show
306 similar trends on large scales. Beyond the alongshore scale of 30 km, the coastline
307 variation is resulted from the cumulative effects of interactions between
308 hydrodynamic forcing and geological features. As it can be seen shoreline of Hainan
309 Island is divided by various protruding headlands into beach sections of different

310 orientations (Figure 1). While the incoming wave direction from South China Sea is
311 fairly uniform in space, the intersection angle of wave is related to the orientation of
312 local shoreline. Consequently, the sections that have different orientations are affected
313 differently by these hydrodynamic conditions. As a result, the coast sections in four
314 different directions can be clearly identified from the wavelet transform results as
315 shown in Figure 6(c).

316

317 **Conclusions**

318 Based on the shoreline change data collected at Hainan Island over a 13-month
319 period the analysis reveals that the power-law relationships between the mean
320 variance and the length scale of the annual shoreline changes can hold up to an
321 alongshore scale of 30 km which is several times greater than that has been found in
322 the previous studies⁸. While there is no spatial pattern within the wave direction or
323 significant wave height along the studied coast, the hydrodynamic conditions show
324 significant seasonal character. Five tropical cyclones showed strong impacts on east
325 and south coasts of Hainan Island, and diminished the shoreline change patterns with
326 alongshore scale of 10-25 km. Much of the effects on the shoreline evolution caused
327 by the storm can get averaged out over a time scale of one year, as the long-term
328 shoreline evolution is mostly a diffusive process with diminishing memory effects
329 with time²³. In the time period of one year, the shoreline change patterns develop into
330 larger spatial scale than seasonal shoreline change patterns, but it is confined by
331 relatively closed bays at scale around 30 km. Furthermore, the coastal orientation

332 changes are also found to be effective in alongshore scale from 40 km to 80 km, or
333 even larger.

334 It should be pointed out that the shoreline change behavior described has limits as
335 it is based on a coarsely sampled shoreline data from only three surveys over a 13
336 month period. The results obtained may contain some degrees of uncertainty and are
337 inevitably influenced by the particular morphological characteristics of Hainan Island.
338 More sites with different coastal conditions and data resolutions (spatial and temporal)
339 should be investigated to further establish the scale relationships of shoreline changes
340 on wave-dominated sandy coasts and underlying mechanisms for these changes.

341

342 **Acknowledgments**

343 This study is carried out as part of a larger project funded by the Public Science
344 and Technology Research Funds Projects of Ocean, China (Grant no. 201405037).
345 The data sets are provided by State Key Laboratory of Estuarine and Coastal Research,
346 ECNU, and requests for materials should be addressed to Shenliang Chen
347 (slchen@sklec.ecnu.edu.cn). The financial support through a joint PhD program
348 awarded to Xiaojing Zhong by the Chinese Scholarship Council and University of
349 Dundee, UK is gratefully acknowledged. The authors would like to thank Jin Hu,
350 Weiheng Zheng, Qing Chen and Wufeng Cheng for their contributions in the field
351 work.

352

353

References:

354 1. Werner, B.T. and Fink, T.M., Beach cusps as self-organized patterns. *Science*, **1993**, 260, pp.

- 355 968-71.
- 356 2. Garnier, R., Dodd, N., Falqués, A. and Calvete, D., Mechanisms controlling crescentic bar
357 amplitude. *J. Geophys. Res.*, **2010**, 115.
- 358 3. Tiessen, M.C.H., Dodd, N. and Garnier, R., Development of crescentic bars for a periodically
359 perturbed initial bathymetry. *J. Geophys. Res.*, **2011**, 116.
- 360 4. Dong, P., Chen, Y.Q. and Chen, S.L., Sediment size effects on rip channel dynamics. *Coast. Eng.*,
361 **2015**, pp. 124-135.
- 362 5. Ashton, A.D. and Murray, A.B., High-angle wave instability and emergent shoreline shapes: 1.
363 Modeling of sand waves, flying spits, and capes. *J. Geophys. Res.*, **2006**, 111.
- 364 6. Lazarus, E.D. and Armstrong, S., Self-organized pattern formation in coastal barrier washover
365 deposits. *Geology*, **2015**, 43, pp. 363-366.
- 366 7. Tebbens, S.F., Burroughs, S.M. and Nelson, E.E., Wavelet analysis of shoreline change on the
367 Outer Banks of North Carolina: an example of complexity in the marine sciences. *Proceedings of the*
368 *National Academy of Sciences*, **2002**, 99(suppl 1), pp. 2554-2560.
- 369 8. Lazarus, E., Ashton, A., Murray, A.B., Tebbens, S. and Burroughs, S., Cumulative versus transient
370 shoreline change: Dependencies on temporal and spatial scale. *J. Geophys. Res.*, **2011**, 116.
- 371 9. Baas, A.C., Chaos, fractals and self-organization in coastal geomorphology: simulating dune
372 landscapes in vegetated environments. *Geomorphology*, **2002**, 48, pp. 309-328.
- 373 10. Southgate, H.N. and Möller, I., Fractal properties of coastal profile evolution at Duck, North
374 Carolina. *Journal of Geophysical Research: Oceans*, **2000**, 105, pp. 11489-11507.
- 375 11. Yang, Z.H., Jia, J.J., Wang, X.K. and Gao, J.H., Characteristics and variations of water and
376 sediment fluxes into the sea of the top three rivers of Hainan in recent 50 years. *Marine Science*
377 *Bulletin*, **2013**, 32, pp. 92-99.
- 378 12. Wang, B., Chen, S., Gong, W., Lin, W. and Xu, Y., *Formation and evolution of the embayment*
379 *coasts around Hainan Island*, Ocean Press: Beijing **2006**.
- 380 13. Tchernia, P., *Descriptive Regional Oceanography*, Pergamon Press: Oxford, New York **1980**.
- 381 14. Zhang, K., Song, C. and Chen, Y., Records and disaster evaluation of typhoons in east Hainan
382 Island in recent 50 years., **2010**.
- 383 15. Boak, E.H. and Turner, I.L., Shoreline definition and detection: A review. *J. Coastal Res.*, **2005**,
384 214, pp. 688-703.
- 385 16. Friedman, G.M., Dynamic processes and statistical parameters compared for size frequency
386 distribution of beach and river sands. *J. Sediment. Res.*, **1967**, 37, pp. 327-354.
- 387 17. Vincent, L., Dolan, R., Hayden, B. and Resio, D., Systematic variations in barrier-island
388 topography. *The Journal of Geology*, **1976**, 84, pp. 583-594.
- 389 18. Zhou, L.M., Li, Z.B., Lin, M. and Wang, A.F., Numerical simulation of wave field in the South
390 China Sea using WAVEWATCH III. *Chin. J. Oceanol. Limn.*, **2014**, 32, pp. 656-664.
- 391 19. Del Río, L., Gracia, F.J. and Benavente, J., Shoreline change patterns in sandy coasts. A case study
392 in SW Spain. *Geomorphology*, **2013**, 196, pp. 252-266.
- 393 20. Coco, G. and Murray, A.B., Patterns in the sand: From forcing templates to self-organization.
394 *Geomorphology*, **2007**, 91, pp. 271-290.
- 395 21. Murray, A.B., Lazarus, E., Ashton, A., Baas, A., Coco, G., Coulthard, T., Fonstad, M., Haff, P.,
396 McNamara, D., Paola, C., Pelletier, J. and Reinhardt, L., Geomorphology, complexity, and the
397 emerging science of the Earth's surface. *Geomorphology*, **2009**, 103, pp. 496-505.
- 398 22. Jackson, D.W.T., Cooper, J.A.G. and Del Rio, L., Geological control of beach morphodynamic state.

399 *Mar. Geol.*, **2005**, *216*, pp. 297-314.
400 23. Dong, P. and Chen, H., Wave chronology effects on long-term shoreline erosion predictions.
401 *Journal of Waterway, Port, Coast, and Ocean Engineering*, **2001**, *127*, pp. 186-189.
402
403

404 **Table 1** Major capes, rivers along coast of Hainan Island (*based on Yang et al.,
 405 2013).

| Type | Water Discharge* | Sediment Discharge* | Name | Flank Profiles |
|-------|---|---------------------------|-----------------|----------------|
| River | 5.673×10 ⁹ m ³ /y | 3.877×10 ⁵ t/y | Nandu | N002, N003 |
| Cape | | | Hainanjiao | N010, N011 |
| Cape | | | Jingxin (Baohu) | N017, N018 |
| Cape | | | Tonggu | N024, N025 |
| River | 4.780×10 ⁹ m ³ /y | 4.533×10 ⁵ t/y | Wanquan | N039, N040 |
| Cape | | | Dahua | N047, N048 |
| Cape | | | Maliu (Niumiao) | N051, N052 |
| Cape | | | Lingshui | N061, N062 |
| Cape | | | Zhuwanxia | N068, N069 |
| Cape | | | Luhuitou | N069, N070 |
| Cape | | | Nanshan | N077, N078 |
| Cape | | | Yinggeju | N088, N089 |
| River | 3.643×10 ⁹ m ³ /y | 6.989×10 ⁵ t/y | Changhua | N105, N106 |
| Cape | | | Lingao | N125, N126 |

406

407 **Table 2** Contributions of the first and second eigenvectors at different coast sections.

| | Profiles | May2013 | Dec2013 | June2014 |
|--|-----------|---------|---------|----------|
| Contribution of First Eigenvector (%) | N001~N132 | 87 | 88 | 89 |
| | N010~N049 | 82 | 82 | 86 |
| | N049~N087 | 89 | 90 | 91 |
| | N088~N009 | 86 | 89 | 85 |
| Contribution of First and Second Eigenvectors (%) | N001~N132 | 95 | 96 | 96 |
| | N010~N049 | 91 | 93 | 95 |
| | N049~N087 | 96 | 98 | 97 |
| | N088~N009 | 95 | 96 | 95 |

408

409 **Table 3** Parameters of tropical cyclones passed Hainan Island during investigated
 410 period (based on Best Track Data by RSMC Tokyo – Typhoon Center).

| Tropical Cyclone | Maximum sustained wind speed (knot) | Minimum central pressure (hPa) | The longest radius of 30kt winds or greater (nautical mile) | The shortest radius of 30kt winds or greater (nautical mile) |
|------------------|-------------------------------------|--------------------------------|---|--|
| BEBINCA | 40 | 990 | 150 | 120 |
| RUMBIA | 50 | 985 | 180 | 150 |
| JEBI | 50 | 985 | 250 | 150 |
| MANGKHUT | 40 | 992 | 120 | 120 |
| HAIYAN | 125 | 895 | 270 | 180 |

411

412 **Figure 1.** Location map of Hainan Island, wave direction contribution around Hainan and
413 routes of tropical cyclones during the investigated period, particle size (D_{50}) of intertidal
414 sediment collected in May 2013 and profile positions. Profiles are numbered N001 to N132
415 clockwise along the coastline.

416

417 **Figure 2.** Shoreline change around Hainan Island and the results of wavelet analysis. (a)
418 Seasonal shoreline change of May2013-Dec2013 and Dec2013-Jun2014. The ordinate axis
419 indicates shoreline change (negative values - erosion). (b) Wavelet transform results of seasonal
420 shoreline change data with scale parameter $a=1$. (c) Wavelet transform results of seasonal and
421 annual shoreline change data with scale parameters $a=4$ and 16 . The shaded parts are profiles
422 from N010 to N087 (east and south coasts).

423

424 **Figure 3.** Log-log plots (left) and the corresponding power-spectral exponent β (right) relating
425 wavelet coefficient mean variance of shoreline change to alongshore scale, for profiles N010 to
426 N087. Wavelet width is multiplied by 5 kilometers (distance between every two profiles) to get
427 the alongshore scaling.

428

429 **Figure 4.** EOF analysis of beach profiles around Hainan Island. (a) The weightings of the first
430 and second eigenvectors on each profile in three surveys. (b) First eigenvector of beach profiles.
431 (c) Second eigenvector of beach profiles.

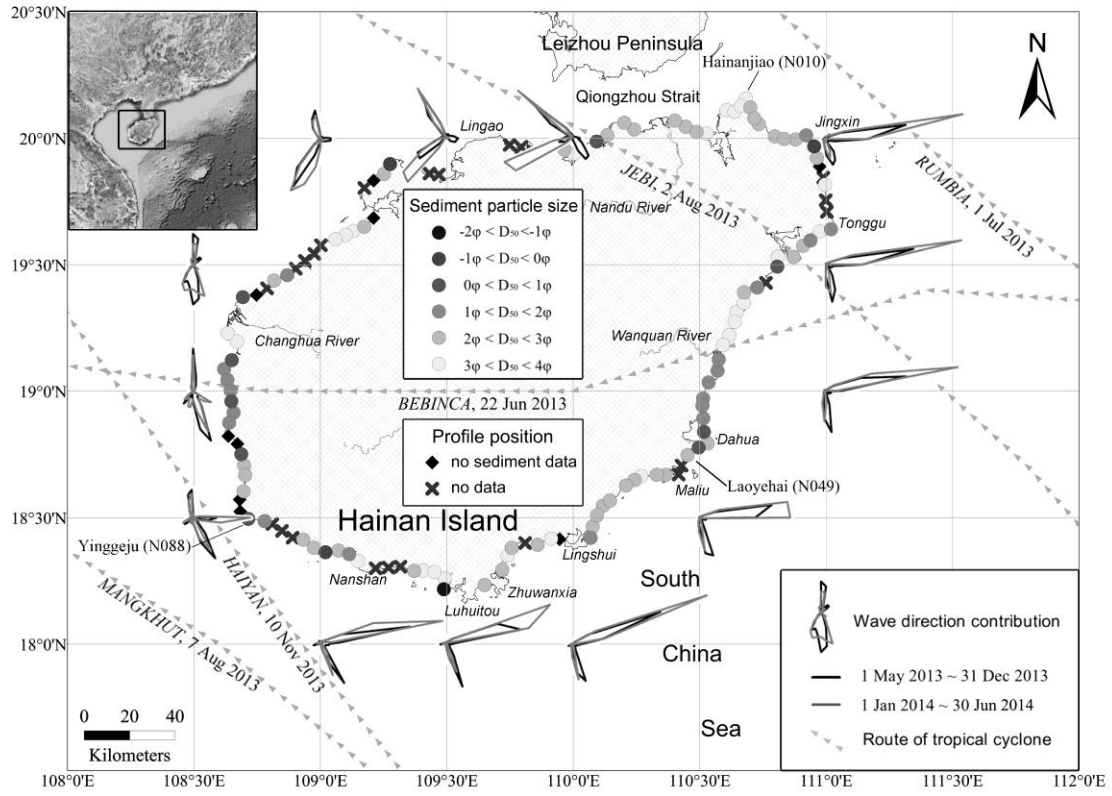
432

433 **Figure 5.** Model results of wave conditions around Hainan. (a) Seasonal significant wave
434 height distribution around Hainan Island, modeled by Zhou *et al.* (2014). (b) and (c) Wave
435 direction and significant wave height at 18.5°N, 110.5 °E (southeast of Hainan) and at 19°N,
436 108.5 °E (west of Hainan) during survey period, modeled by WaveWatch III (WW3) Global
437 Wave Model.

438

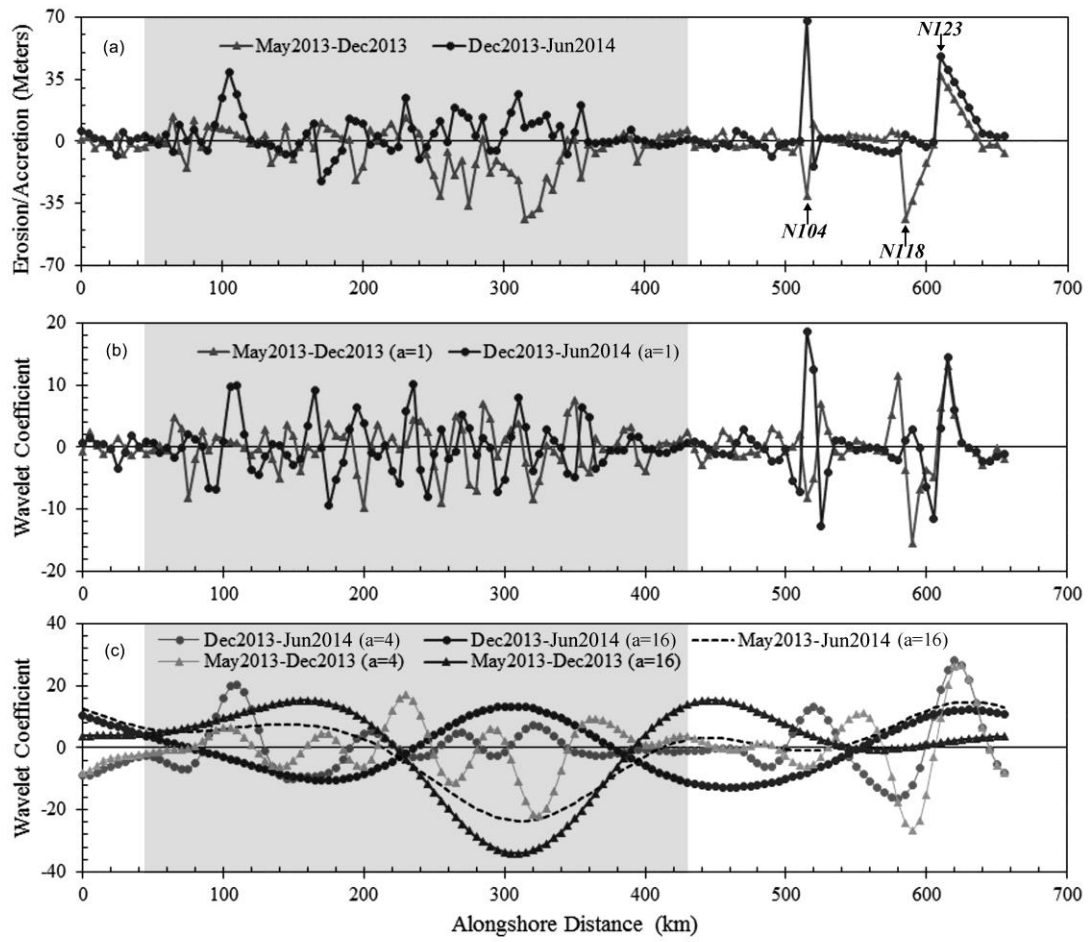
439 **Figure 6.** Wavelet analysis of annual shoreline change, azimuth and submerged slope of
440 alongshore profiles. Wavelet coefficients of azimuth are divided by three for plotting in figures.
441 Submerged slope is calculated between elevations 0 and -5 m at each profile.

442



443
 444
 445

Figure 1



446

447

448

Figure 2

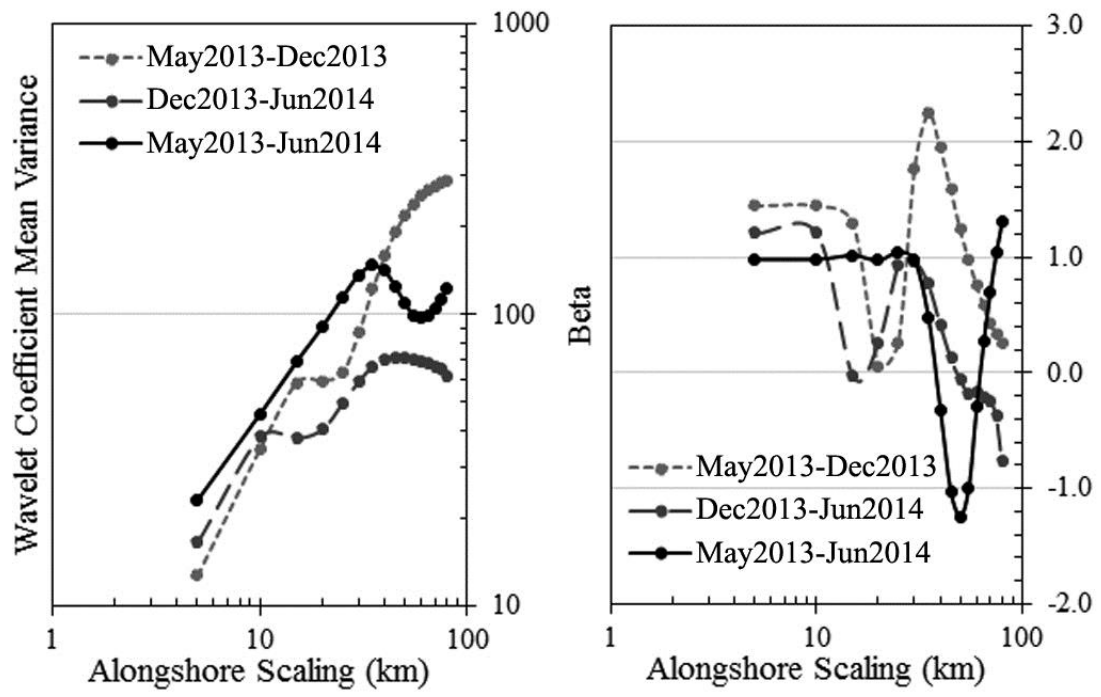
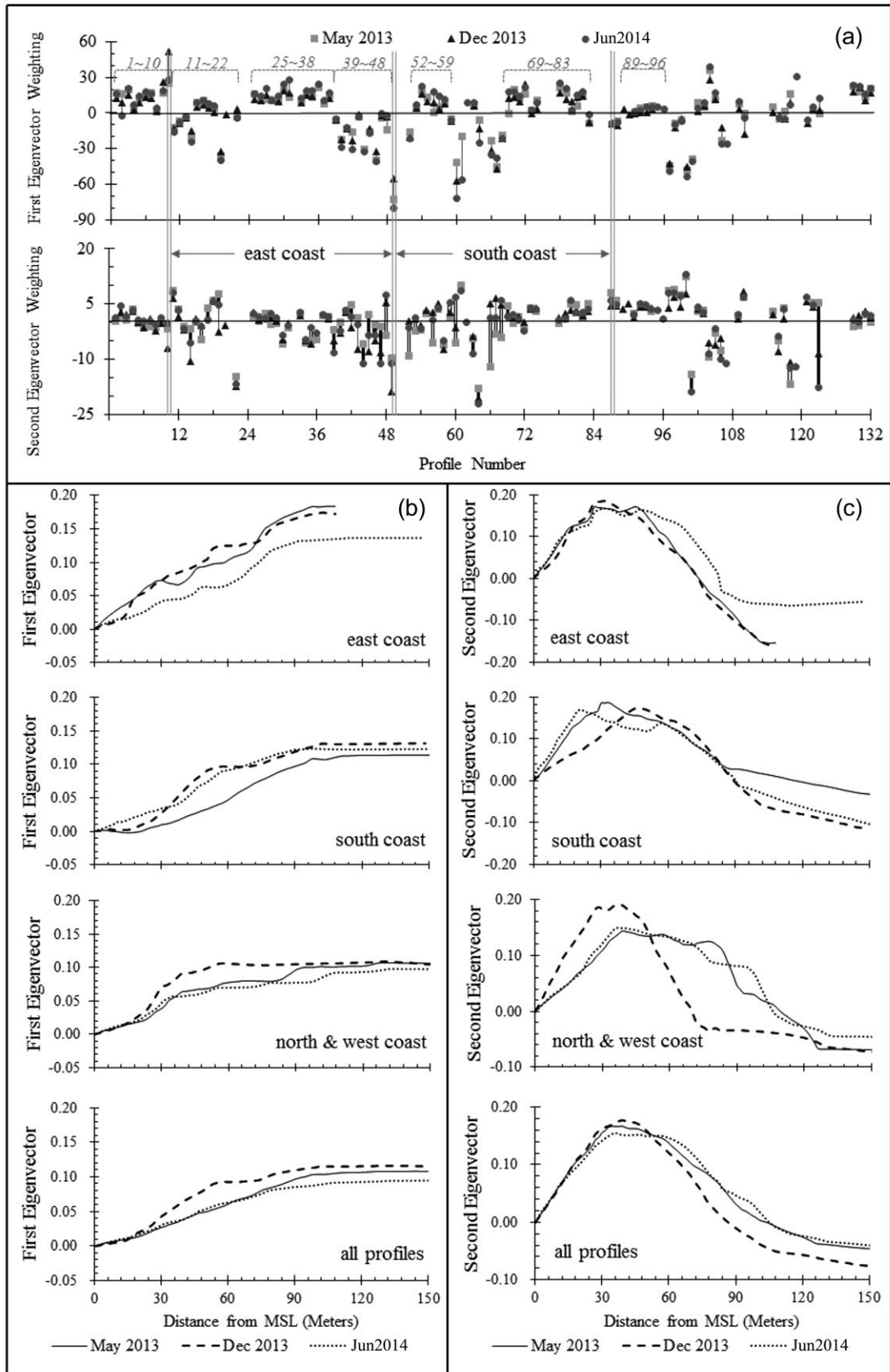


Figure 3

449
 450
 451



452
453
454

Figure 4

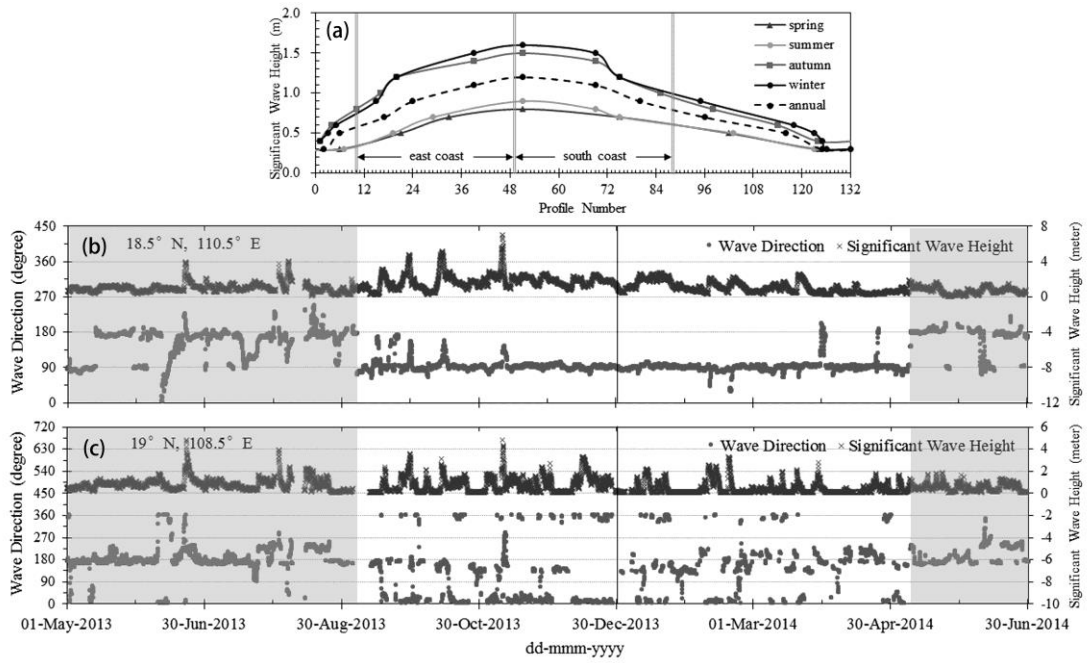
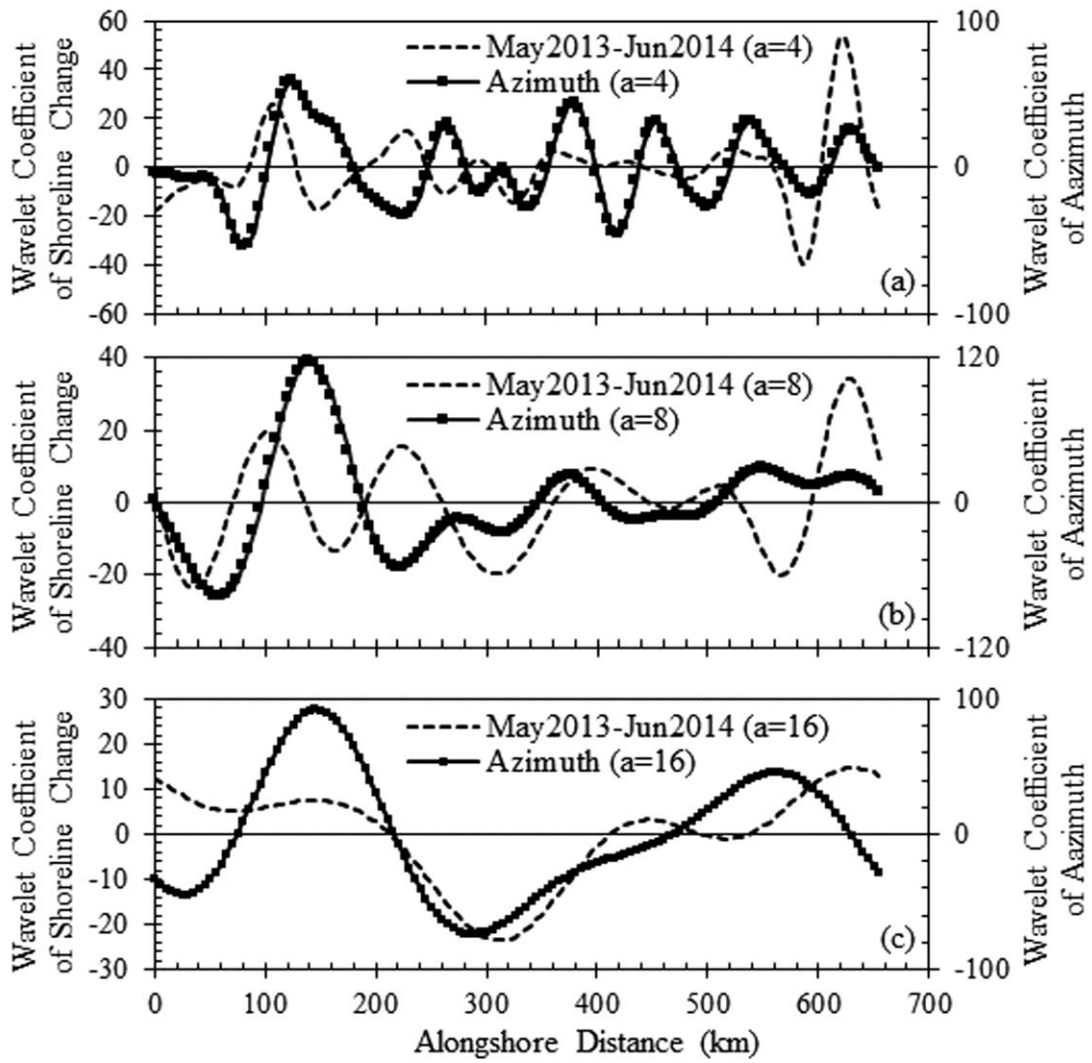


Figure 5

455
456
457



458

459

460

Figure 6